Cryobiology 58 (2009) 157–165

Contents lists available at ScienceDirect

Cryobiology

journal homepage: www.elsevier.com/locate/ycryo

Intracellular ice formation in yeast cells vs. cooling rate: Predictions from modeling vs. experimental observations by differential scanning calorimetry ☆

Shinsuke Seki [a], F.W. Kleinhans [a,b], Peter Mazur [a,*]

[a] Fundamental and Applied Cryobiology Group, Department of Biochemistry and Cellular and Molecular Biology, The University of Tennessee, Knoxville, TN 37932-2575, USA
[b] Department of Physics, Indiana University–Purdue University at Indianapolis, IN 46202, USA

ARTICLE INFO

Article history:
Received 19 August 2008
Accepted 28 November 2008
Available online 11 December 2008

Keywords:
Freezing
Cryobiology
Intracellular ice formation
DSC
Modeling
Yeast

ABSTRACT

To survive freezing, cells must not undergo internal ice formation during cooling. One vital factor is the cooling rate. The faster cells are cooled, the more their contents supercool, and at some subzero temperature that supercooled cytoplasm will freeze. The question is at what temperature? The relation between cooling rate and cell supercooling can be computed. Two important parameters are the water permeability (Lp) and its temperature dependence. To avoid intracellular ice formation (IIF), the supercooling must be eliminated by dehydration before the cell cools to its ice nucleation temperature. With an observed nucleation temperature of −25 °C, the modeling predicts that IIF should not occur in yeast cooled at <20 °C/min and it should occur with near certainty in cells cooled at ⩾30 °C/min. Experiments with differential scanning calorimetry (DSC) confirmed these predictions closely. The premise with the DSC is that if there is no IIF, one should see only a single exotherm representing the freezing of the external water. If IIF occurs, one should see a second, lower temperature exotherm. A further test of whether this second exotherm is IIF is whether it disappears on repeated freezing. IIF disrupts the plasma membrane; consequently, in a subsequent freeze cycle, the cell can no longer supercool and will not exhibit a second exotherm. This proved to be the case at cooling rates >20 °C/min.

Introduction

The formation of ice crystals within cells (IIF) is lethal. The classical approach to avoiding it is to cool cells slowly enough to remove nearly all the potentially freezable cell water osmotically before they have cooled to a temperature that permits the ice nucleation of the supercooled intracellular water. In 1963, Mazur [10] published a physical-chemical model that computes the amount of water remaining in cells as a function of both the subzero temperature and the cooling rate. From those computations and from knowledge or estimates of the cell ice nucleation temperature, one can predict the probability of intracellular freezing as a function of cooling rate.

One direct experimental test of these predictions is to observe under the microscope the percentages of cells that undergo IIF when cooled at various rates. A second, inferential, test is to determine the viability of the cell as a function of cooling rate. If IIF is lethal, then one expects a close coupling between the cooling rates observed to produce IIF and the cooling rates observed to cause a high percentage of killing. There are only a few cell types for which there exist predictions from modeling as well as data from these two sorts of experimental measures. Chief of these are preimplantation mammalian oocytes and embryos [26,13, Fig. 1.10]. And in that case, the agreement among all three is excellent. The triad is reasonably complete for human lymphocytes [24], and the agreement is again good. In the case of the yeast *Saccharomyces cerevisiae*, there is knowledge on their viability as a function of cooling rate [16] and there are predictions from physical-chemical models as to the degree of water loss as a function of temperature and cooling rate [10,7,25]. But except for fragmentary information from freeze-cleaved cells that shows IIF occurring in cells cooled at 55 and 100 °C/min but not in those cooled at 6 or 10 °C/min [1,21], there have been no experimental determinations of the fraction of the yeast cells that undergo IIF as a function of cooling rate and there is no information on the temperature at which IIF occurs. The purpose of the studies reported here was to eliminate this major knowledge gap. One problem is that yeast cells, at least in our hands, do not exhibit the sudden opacity (flashing) that is the usual hallmark of IIF, probably because the cells are too small. Consequently, in this study we turned to differential scanning calorimetry (DSC) to provide the answers.

Materials and methods

Yeast

Subcultures of *S. cerevisiae*, diploid strain NRRL-Y-2235, were prepared as described elsewhere [8] by incubating for 24 h at 25 °C in liquid medium in Erlenmeyer flasks on a shaker (172 cy-

☆ *Statement of funding:* Research supported by NIH Grant R01-RR18470.
* Corresponding author. Fax: +1 865 974 8027.
E-mail address: pmazur@utk.edu (P. Mazur).

0011-2240/$ - see front matter © 2008 Elsevier Inc. All rights reserved.
doi:10.1016/j.cryobiol.2008.11.011

cles/min). The formula for the liquid medium is; glucose 20 g; $(NH_4)_2SO_4$, 3.0 g; KH_2PO_4, 3.0 g; $MgSO_47H_2O$, 0.25 g; $CaCl_22H_2O$, 0.25 g; monosodium glutamate, 1.0 g; yeast extract, 0.1 g; distilled water to make 1000 ml. After incubation, one or two 10-ml aliquots of the Erlenmeyer culture were centrifuged at 500*g* for 5 min, the supernatant was decanted, and the cells were washed twice by centrifugation and decantation with 10 to 12 ml volume of distilled water containing 10 mg/L Snomax (a commercial preparation of freeze-dried *Pseudomanas syringii*, the ice nucleating bacterium [York Snow, Victor, NY]). Snomax is introduced to minimize the supercooling of the suspending medium. After final aspiration of most of the supernatant, the cell concentration in the residual slurry was on the order of 1.0×10^{10} cells per ml as estimated by hemocytometer counts. This slurry was used for the experiments. The cells (excluding buds) average 5.74 μm in diameter [9] and have a mean volume of 99.0 μm^3 .

Several parallel preparations were used to estimate the cytocrit of the slurry. A column of the slurry was introduced into a hematocrit capillary, one end of the capillary sealed with Clay–Adams seal-ease (Parsippany, NY), and the capillary spun at 13,000*g* in a Clay–Adams hematocrit centrifuge for 5 min. The length of the column of packed cells was then measured as a fraction of the length of the whole column.

For experiments, a 1.5–3.8 mg aliquot of the slurry was transferred to the DSC sample cup, which was crimped closed with a lid. Then, just prior to placing the pan in the head of the DSC, the pan was gently inverted and then turned upright. The reason was to remove tiny droplets of water that had condensed on the inner surface of the lid during equilibration. If these droplets were not removed, they often produced a small spurious exotherm as they froze during cooling. The sealed pan was allowed to thermally equilibrate a couple of minutes in the DSC, and the cooling run then begun. The cell suspensions were cooled to −50 or −70 °C at various rates (2, 5, 10, 20, 30, 40, 50, 100 °C/min) inserted into the programmable DSC system.

DSC

A Perkin–Elmer (PE) DSC-7 differential scanning calorimeter and PE Thermal Analysis Software, Ver. 2.20, running under a Unix operating system, a PE Liquid Nitrogen Subambient Accessory, and PE crimpable aluminum sample pans (#0219-0062) were used for all the DSC experiments as described elsewhere [6]. Because of thermal lag between the actual sample temperature in the DSC and the observed platinum resistance thermometer read out, it is necessary to apply a correction factor [6,2,5,18]. Temperature calibration of the DSC for such studies is non-trivial. For these studies, we required DSC cooling rates up to 100 °C/min. The standard procedure for calibrating a DSC, including the DSC-7, is to calibrate to the melting point of a known standard or standards in the temperature range of interest and at the temperature scan speed of interest. We typically calibrate our DSC in the range of −100 °C to +20 °C at a warming rate (scan rate) of 10 °C/min. At other scan speeds other uncorrected thermal offsets arise between the true temperature of the sample and the DSC readout. These offsets must be measured and applied to the DSC temperature readout. Determining the offsets for warming runs is relatively easy. The true melting point of a standard sample does not depend on the warming rate. Thus any observed difference between the true and measured melting point is due to the offset (typically, lag) between the sample and the DSC temperature readout. Calibration of cooling runs is more complex. At high cooling rates two problems occur. First, the true sample temperature increasingly lags the readout temperature. Second, the standards typically undergo supercooling and do not freeze at their thermodynamic freezing point, but rather at some lower temperature. The degree of supercooling is an unknown which complicates the calibration process.

In a previous report [6], we calculated the formula to correct the thermal lag at scan rates of 0.5–20 °C/min. However, in this study, we varied the scan rates from 2 to 100 °C/min and so needed to recalibrate the DSC. This repeat calibration used the freezing/melting phase transition of distilled water (0 °C), cyclohexane (6.54 and −87.06 °C), and *n*-decane (−29.66 °C). Samples were scanned at rates of ±4 to ±150 °C/min. Freezing points were defined as the onset temperature of an exotherm, and melting points were defined as the onset temperature of the endotherm. Fig. 1 shows the exothermograms for the freezing of *n*-decane cooled at rates of 4–150 °C/min. The thermodynamic freezing point of *n*-decane is −29.66 °C; however, the onset temperatures of the freezing exotherm were lower and the discrepancy increased with increasing cooling rate. From these data, the temperature correction (T_c) to the observed DSC temperatures, for a given cooling rate (CR) or warming rate (WR), was determined to be:

$$\text{During warming, } T_c = 0.600\ ^\circ\text{C} - [(\text{WR}) - (10\ ^\circ\text{C/min})] \times (0.070\ (^\circ\text{C})/(^\circ\text{C/min})) \quad (1)$$

$$\text{During cooling, } T_c = 0.600\ ^\circ\text{C} + (10\ ^\circ\text{C/min})(0.070\ ^\circ\text{C}/^\circ\text{C/min}) + (\text{CR})(0.080\ (^\circ\text{C})/(^\circ\text{C/min})) \quad (2)$$

Here in more detail is the procedure for using the above formulas to correct for the thermal lag. First the DSC is calibrated per the user's manual at a warming rate of 10 °C/min. After calibration, a residual temperature error of 0.6 °C remained (unrelated to scan rate) which we incorporate into our overall temperature correction. Second, the standards are scanned at rates between +4 and +150 °C/min and the offset in melting points yields a thermal lag correction of 0.070 (°C)/(°C/min) [Eq. (1)]. Finally, the standards are cooled at rates up to 150 °C/min. Because of supercooling, we do not know at what temperature the standards should freeze. However, we assume that the degree of supercooling is only weakly dependent on the cooling rate (which empirically appears to be true for the standards we use). Thus, we adjust the thermal lag term in our temperature correction formula (Eq. (2)) to yield a freezing point which is independent of the cooling rate. This freezing point will be below the thermodynamic freezing point because of supercooling. As a check on this method, we expect (i) to get the same lag coefficient independent of the standard used and (ii) to obtain nearly the same lag during cooling as during warming (since the thermal inertia of the machine should be independent of whether warming or cooling is occurring). Fig. 2A shows the measured freezing points of water, *n*-decane, and cyclohexane and

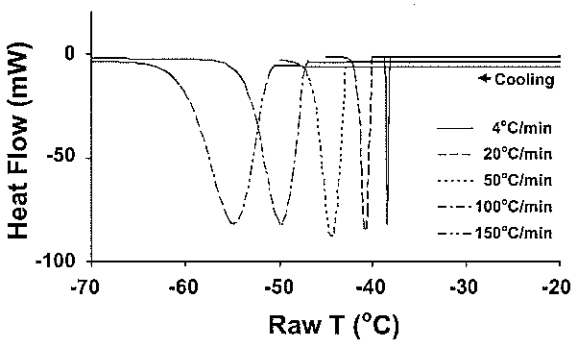

Fig. 1. Effect of DSC scan rate on the temperature of the freezing exotherm of *n*-decane. The true freezing point of *n*-decane is −29.6 °C; consequently, scan rate corrections must be applied to convert the measured temperatures to true temperatures.

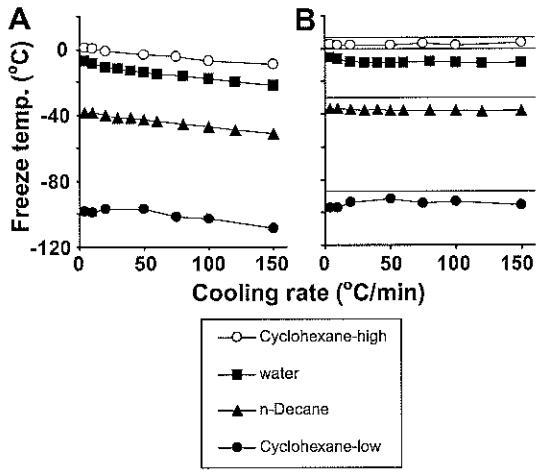

Fig. 2. The freezing temperatures of water, *n*-decane, and cyclohexane as a function of cooling rate (= scan rate): (A) Based on observed temperatures in the DSC. (B) Based on temperatures corrected for thermal lags (see text). The horizontal lines just above the data points are the known melting points of the respective test samples.

Fig. 2B shows their corrected freezing points with a cooling lag coefficient of 0.08 (°C)/(°C/min). As expected, a single correction coefficient works for all the standards, suggesting that the results are not being significantly confounded by supercooling issues. Furthermore, the correction coefficient for cooling is almost identical to that found for warming (0.08 vs. 0.07). For all these reasons, we believe we can reliably and accurately measure true sample temperatures at cooling rates up to 150 °C/min.

It was often desirable to quantify the heat released during the freezing of the yeast cells. This requires determining the area under the IIF peaks. The area will have units of the product of the *X* and *Y* axes. The *X* axis is actually a time axis which the PE software automatically converts to temperature on the basis of the sweep rate. Thus, the units of area are:

$$X * Y = (\delta T/S_{wp})\ \text{Rate}) \times (\text{mW}) = (^{\circ}\text{C})/(^{\circ}\text{C/s}) \times (\text{mJ/s}) = \text{mJ}. \quad (3)$$

The PE software can compute these areas (energies).

In Fig. 1, the widths of the exotherm peaks, and hence the areas under them, increase markedly as the scan rate (cooling rate) increases. This is in a sense an artifact resulting from the fact that Fig. 1 plots heat flow in units of power (mW) vs. temperature. As indicated in Eq. (3), the energy released during the exotherm is the area under the curve of a plot of heat flow vs. time, with time being equal to temperature divided by the cooling or scan rate.

Modeling and the prediction of IIF in yeast cells as a function of cooling rate

The thermodynamic freezing point of most cells (the highest temperature at which ice can co-exist with the protoplasmic solution) is about −0.5 °C. But cells do not freeze even in the presence of external ice unless the temperature falls from 5 to 40 °C below that temperature. By definition, water below its freezing point is supercooled. And supercooled water has a higher vapor pressure, activity, or chemical potential at a given subzero temperature than that of ice or that of water in a solution in equilibrium with ice. The consequence is that as long as the cell contents remain supercooled, the resulting vapor pressure or chemical potential difference will provide a driving force for intracellular water to leave the cell and freeze externally. In other words, the cell will tend to dehydrate during cooling. The rate and extent of that dehydration depends primarily on two variables. One is the inherent permeability of the cell to water; i.e., the hydraulic conductivity, Lp. The other is the cooling rate. For a cell of given Lp, the slower it is cooled, the more it is able to lose sufficient water to remain in near chemical potential equilibrium with external ice and solution, and conversely, the faster it is cooled, the less it is able to dehydrate and the more its water will become supercooled as the temperature falls.

This qualitative description can be described quantitatively by four coupled equations [10,14]. The first equation relates the rate of loss of cytoplasmic water to the difference in chemical potentials of intracellular and extracellular water expressed as a vapor pressure ratio; i.e.

$$dV/dt = (\text{Lp}ART\ \ln p_e/p_i)/v_w, \quad (4)$$

where V is the volume of cell water, t is time, Lp is the permeability coefficient for water (hydraulic conductivity), A is the cell surface area, R the gas constant (μm³ atm/deg mol), and v_w is the molar volume of water. The ratio p_e/p_i is that for the external and internal vapor pressures of water. It is <1 because the intracellular water is supercooled, and the vapor pressure of supercooled water is greater than that of ice or of water in a solution in equilibrium with ice. The change in this vapor pressure ratio with temperature can be calculated from a second differential equation derived from the Clausius–Clapeyron relation and Raoult's law:

$$d\ln(p_e/p_i)/dT = L_f/RT^2 - [N_2 v_w/((V + N_2 v_w)V)]dV/dT \quad (5)$$

Here, N_2 is osmoles of solute in the cell and L_f is the molar latent heat of fusion of ice.

Time and temperature are related by the cooling rate, which if linear, is given by

$$dT/dt = B \quad (6)$$

Finally, the hydraulic conductivity, Lp, decreases with falling temperature. If it is assumed to follow an Arrhenius relation, its value at a given absolute temperature, T, is given by

$$\text{Lp} = \text{Lp}_g \exp\{-Ea/R'[(1/T) - (1/T_g)]\}, \quad (7)$$

where the subscript g refers to the value at a given reference temperature (usually 20 °C or 0 °C), and R' is the gas constant, here expressed in the units cal/deg mol. Ea is the activation energy of Lp in cal/mol. R, R', L_f, and v_w are constants, the values of which are given

Table 1
Parameters and constants for calculating water loss of yeast cells during freezing at various rates.

Item	Symbol	Value	Units
Osmolality of cytoplasm	M_i	0.5	Osmolal
Freezing point of cytoplasm	T_f	272	K
Vol. of water in isotonic cell	V_i^o	88	μm³
Initial vol. of cell water at $T = T_f$	V_i	88	μm³
Vol. of cell water at T	V	—	μm³
Rel. Vol. of cell water at T	V/V_i	—	—
Osmoles of solute in cell	N_2	4.4×10^{-14}	Osmoles
Hydraulic conductivity at 20 °C	Lp_g	0.105*	μm/min/atm
Activation energy of Lp	Ea	13.5*	kcal/mol
Area of cell protoplast	A	107	μm²
Gas constant	R	82.057×10^{12}	μm³ atm/(mol deg)
	R'	1.987	cal/mol deg
Molar volume of water	V_w	18×10^{12}	μm³/mol
Molar heat of fusion	L_f	5.95×10^{16}	μm³ atm/mol
Cooling rates	B	2–100	°C/min
Temperatures	T	272–233	K

Values for V_i^o, N_2, and A are from [10].
* The Mean Lp and Ea reported by Levin [7] for cooling rates of 10 °C/min and 100 °C/min. Using a DSC approach and a cooling rate of 10 °C/min, Han et al. [4] have found similar values; namely Lp_g (20 °C) = 0.066 μm/min/atm and Ea = 15.9 kcal/mol.

in Table 1. The values of A, N_2, Lp_g, and Ea are constant for a given cell but differ in different cells. Ea may also be a different value below 0 °C than above 0 °C. The values in Table 1 are for yeast cells. Knowledge of Lp_g, Ea, N_2, and A/V_i^o (the surface to volume ratio of the isotonic cell) permit one to compute the volume of cell water (and the extent of supercooling) versus subzero temperature and cooling rate. Eqs. (4)–(7) are solved by the Runge–Kutta method [14], assuming L_f to be constant. Actually, as discussed in the appendix in [10], it decreases with falling temperature, but the effect on the kinetic curves is small.

The thermodynamic situation with yeast is atypical since the cells are suspended in "pure" water. The ratio p_e/p_i in Eqs. 4 and 5 is a measure of the difference between the chemical potentials of the external water and that of intracellular water. For the pure water in the external medium, its chemical potential is

$$\mu_w^e = \mu_w^o \tag{8}$$

For the water in the solution comprising the protoplasm of a yeast cell, at first consideration, its chemical potential is

$$\mu_w^i = \mu_w^o + RT \ln a_w^i, \tag{9}$$

where a_w^i, the activity of the water, is the vapor pressure of water in the cell solution/vapor pressure of pure water. In the cell, $p_i < p_w^o$ because p_i is suppressed by the presence of cell solutes. Consequently, ln a_w is negative. With these two equations, there is no way to make $\mu_w^i = \mu_w^e$. If an animal cell is placed in distilled water, it will continue to take up water in a futile effort to increase its vapor pressure until it lyses. But in yeast, which posses an elastic cell wall, and higher plant cells, which have a rigid cell wall, the initial entry of water causes the protoplast to press against the cell wall, and this creates a hydrostatic pressure. The hydrostatic pressure (P) increases the chemical potential of water as

$$\mu_w^i = \mu_w^o + RT \ln a_w + v_w P, \tag{9a}$$

where v_w is the partial molal volume of water. Since a_w is <1, RT ln a_w is negative. Consequently, μ_w^i and μ_w^e become equal in Eqs. (8) and (9)a when the hydrostatic term in (9a) becomes equal and opposite the activity term. The activity term can also be expressed in terms of osmotic pressure (Π) as $v_w\Pi$, and in terms of osmolality as RTM, where M is the osmolality [13, p. 13]. Thus, when a yeast cell is in equilibrium with pure water, the hydrostatic pressure on the wall equals the osmotic pressure in the cell. Since the intracellular osmolality is 0.5 osmolal, Π (and P) = RT*0.5 = 11.2 atmospheres at equilibrium at 0 °C.

What happens then when the "pure" external water freezes? Below 0 °C, the chemical potential of the external ice drops below that of liquid water at the same temperature; consequently, the chemical potential of the intracellular supercooled water now exceeds that of the ice. In response, an incremental volume of water leaves the cell. This pressure-driven efflux lowers the hydrostatic pressure from the elastic cell wall and it continues until the hydrostatic pressure drops to zero. From that point forward, the yeast cell behaves like any animal cell in that the chemical potential of its intracellular water is determined exclusively by the activity (or osmolality) of the intracellular solution. The crossover temperature occurs when the intracellular hydrostatic pressure drops to zero and the activity of the external ice becomes equal to the activity of the internal solution. We have the relationship that the freezing point of a solution $(T_f) = -M \times 1.86$, where 1.86 is the so-called molal freezing point constant. Since $M = 0.5$, T_f is −0.93 °C. Below this temperature, then, the yeast cell will have lost sufficient water to eliminate any hydrostatic pressure, and Eqs. (4) and (5) will hold.

In reality, the external medium will not be pure water because incomplete washing and leakage of solutes from damaged cells will result in its being a very dilute, hypotonic solution. But that does not affect the basic arguments just presented.

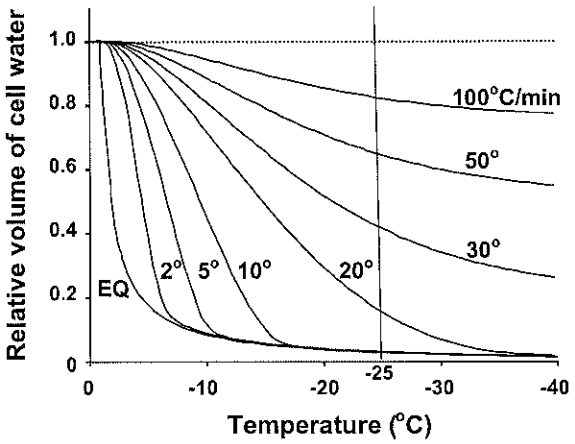

Fig. 3. Computed volumes of water in yeast cells suspended in water and cooled to various temperatures at rates ranging from 2 to 100 °C/min. The curve labeled EQ is the volume of cell water required to keep it in chemical potential equilibrium with the external ice and water. This is equivalent to the volumes of water in cells cooled infinitely slowly. The curves were computed from the equations given in the text. Values of the several constants and adjustable parameters are given in Table 1.

Fig. 3 shows such computations for the yeast *S. cerevisiae* suspended in water. It plots the volume of cell water during freezing as a fraction of the volume of water in the unfrozen cell for cooling rates ranging from 2 to 100 °C/min. It also depicts an equilibrium curve (EQ). It shows the volume of water that a cell has to possess to remain in chemical potential equilibrium with external ice; i.e., the volume of water in a cell that is cooled infinitesimally slowly. That curve is generated by the equation

$$V' = V/V_i = v_w M_i \times 10^{-15} / \exp[L_f/R(1/T - 1/273)] - 1, \tag{10}$$

where V' is the fractional water volume, V_i is the initial water volume, and M_i is the initial osmolality [10].

The higher the cooling rate, the more the curves shift to the right of the equilibrium curve. The number of degrees the curve is shifted is the number of degrees the cell water is supercooled at given temperatures. The vertical line at −25 °C represents a temperature at which a supercooled yeast cell becomes capable of being nucleated. The curves lead to the following predictions; namely, yeast cells cooled at 2 to 10 °C/min should not undergo intracellular ice formation (IIF) because their water volume becomes reduced to the equilibrium value well above the cell nucleation temperature, and therefore that water is no longer supercooled. In contrast, cells cooled at 30, 50, and 100 °C/min or higher should undergo IIF with near certainty because their relative water contents at −25 °C (41, 64, and 82%, respectively) are far above the equilibrium value at −25 °C (3%), and consequently the cells are extensively supercooled at this temperature. The yeast cells cooled at 20 °C/min are predicted to be on the border; they probably ought not to undergo IIF because, by −25 °C, their relative water content has dropped to 15%. Mazur et al. [17, p. 162] have shown that mouse oocytes with their water content reduced to 19.7% of normal do not undergo IIF.

Calorimetric results

There are two basic premises behind these experiments. One is that if the cooling rate is high enough, the water in a yeast cell will become increasingly supercooled with a drop in temperature, and that supercooled water will freeze at a temperature well below the temperature for external ice formation (EIF). Consequently, two exotherms will be generated–one at a high temperature produced by the extracellular freezing and one at a lower temperature pro-

duced by IIF. The second premise is that to maintain a supercooled state, the plasma membrane of the cell must be intact. There is extensive evidence that IIF causes membrane disruption. Therefore, if a cell has undergone IIF and consequent membrane disruption on an initial freeze, it will be unable to supercool on a repeated sequence of cooling, and the low temperature exotherm will vanish. Another way to put this is that prior to an initial IIF, the cell suspension has two compartments—the cell and the medium. But if the membrane is damaged by IIF in the initial freezing, the system then consists only of a single compartment. There can be no intracellular freezing for there no longer is an intracellular compartment. Our experiments, therefore, consisted of subjecting the yeast to four freeze–thaw cycles, with the cooling rate fixed in a given set. A similar approach was used by Bryant [2] to assess IIF in human lymphocytes suspended in 10% Me_2SO.

Exotherms observed as a function of cooling rate

Fig. 4 compares the DSC exothermograms for distilled water and for yeast cells in distilled water cooled to −10 °C at rate of 2 °C/min. In distilled water alone, one sees only a single very sharp freezing peak initiating at −3 °C with a return to the baseline after further cooling of only a couple of tenths of a degree (dashed curve). When yeast are added to the water (solid curve), the main difference is the relatively long shoulder between the start of the rebound and the return to the base line. The modeled 2 °C/min curve in Fig. 3 indicates that with no supercooling of the medium, the cells will be undergoing a rapid loss of water in the range of −2 to −7 °C. Consequently, the most likely explanation is that the shoulder in Fig. 4 represents the heat of fusion released by the freezing of cell water as it flows out into the external medium during cooling. An alternative is that some of that shoulder exotherm is water that has frozen intracellularly. By itself, the DSC can not distinguish between the two possibilities. But what can distinguish between the two mechanisms are the experiments reported in Fig. 5.

Fig. 5A shows the thermograms obtained when a given yeast suspension was subjected to four sequential cycles of cooling at 2 °C/min and thawing. Essentially no change occurs. Except for Cycle I, the temperature of the onset of the exotherm is the same (the variability is typical of that we have observed for ice nucleation by Snomax), and the shape and duration of the shoulder remains unchanged over the cycling. The areas under the shoulder are 58, 55, 56, and 57 J/g during freezing cycles I–IV, respectively. If a significant part of the shoulder were ascribable to IIF, that contribution should disappear with repeated freezing/thawing. (We will elaborate shortly). The results are the same for repeated freezings at 5 °C/min (not shown) and at 10 °C/min (Fig. 5B).

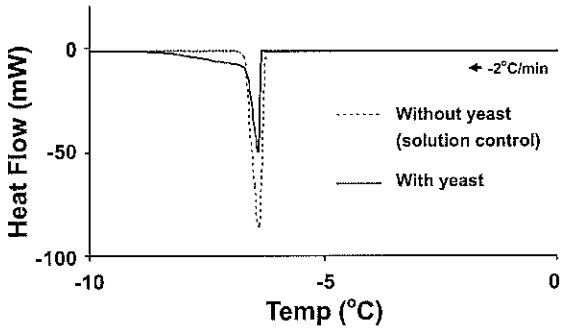

Fig. 4. DSC thermograms of samples of distilled water with yeast cells present (solid line) and without yeast cells present (dotted line). The cooling rate was 2 °C/min.

At 20 °C/min (Fig. 5C), there is a change; namely, the area under the shoulder decreases in moving from cycles I to II, III, and IV from 74 J/g in Cycle I to 34, 26, and 28 J/g in Cycles II, III, and IV. This indicates that some fraction of the shoulder in Cycle I is due to the heat released by IIF. The procedure for computing that fraction is shown in the bottom panel of 5 C. However, there is still no appearance of a second exothermic peak. That changes when the cooling rate is increased to 30, 50, and 100 °C/min. At a cooling rate of 30 °C/min (Fig. 5D), a small separate peak has become visible at −23 °C. That peak disappears by the third freezing cycle. At 50 °C/min (Figs. 5E and 6, top), the second peak is very evident in the first cycle (63 J/g), diminished in the second (25 J/g), and has disappeared in the third and fourth cycle. At 100 °C/min (Fig. 6, bottom), the low temperature peak (which we ascribe to IIF) is nearly as large as the high temperature peak which we ascribe to EIF.

The temperature of IIF in yeast cells

Aside from information on the presence or absence of an IIF peak and its size, the DSC also shows the temperature at which IIF occurs. As shown by Point **d** in Fig. 6B, we define that temperature as the modal point of the low temperature exotherm. Since this exotherm represents the summation of the heat released by some ten billion yeast cells, we believe that the modal temperature is the appropriate measure. For the three cooling rates at which a separate IIF peak was observed (30, 50, and 100 °C/min), the modal temperatures were -22.9 ± 0.4, -23.8 ± 0.8, and -26.6 ± 0.7 °C. The thermograms in Figs. 5 and 6 are examples of individual runs. Each run was repeated 3–5 times with closely similar results.

The Ratio of the heat released by the freezing of cell water to that of the total heat released during freezing (cell water plus the freezing of the external medium)

Table 2 shows the heat released during each of four cycles of freezing of individual samples of yeast suspensions cooled at 2, 20, and 50 °C/min. At the two lower cooling rates, the thermograms consisted of a high temperature exotherm overlapping with an extended lower temperature shoulder (Fig. 5A and C). With cooling at 20 °C/min, the combined total area of the exotherms remained constant at about 212 J/g over the four cycles (Column C). However, the area of the shoulder decreased from 74 to 28 J/g (Column D). As mentioned, we interpret the shoulder to include the freezing of two sorts of cell water. One is the portion that freezes inside the cell; i.e., IIF. The other is water that flows out of the cell during slow cooling and freezes externally. Since IIF disrupts membranes, we expect the former contributor to vanish with repeated freezing. Since the latter occurs only in cells with intact membranes (i.e., those not undergoing IIF), we expect their thermal contribution to remain unchanged with cycling. In this particular example, that contribution is 28 J/g. The contribution then of IIF to the shoulder exotherm will be the values in Cycles I to III of Column D minus the value in Cycle IV. Those are tabulated in Column E. Finally, the ratio of each value in Column E to that in Column C is the fraction of the total exotherm that results from IIF (Column F). It is that fraction or ratio that is plotted in Fig. 7.

With cooling at 2 °C/min, there is no change in the area under the shoulder with repeated freezing cycles (Column D), and therefore, by our reasoning, none of the shoulder is attributable to IIF (column E). The yeast cells cooled at 50 °C/min behaved like those cooled at 20 °C/min with one exception. The exception is that the low temperature exotherm is no longer an appendage shoulder to the high temperature exotherm, but a nearly separate peak (Fig. 6A).

Fig. 7 plots the fraction of the exotherms attributable to IIF for all the conditions studied as a function of (A) the number of freez-

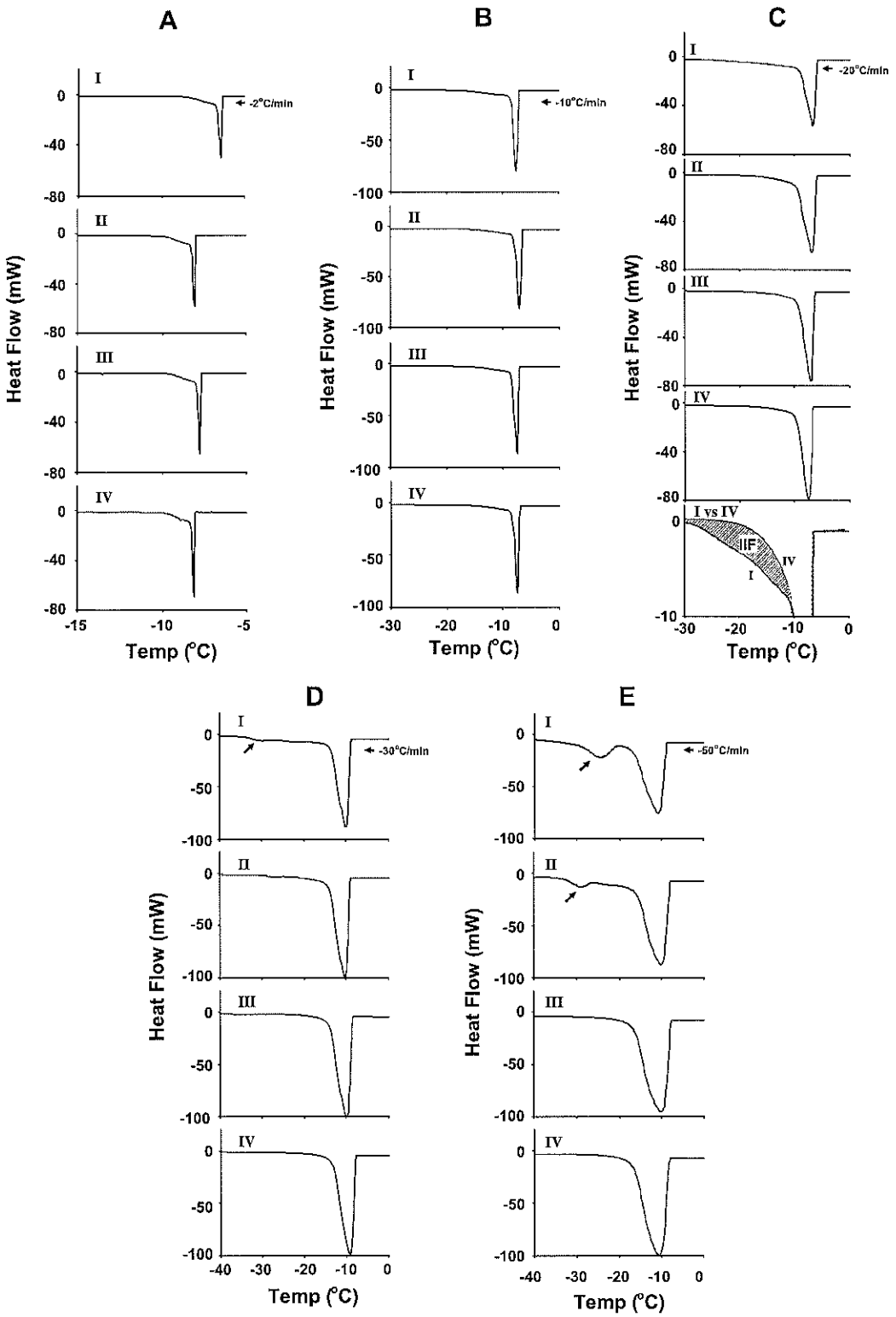

Fig. 5. DSC thermograms of yeast cells in distilled water cooled at 2 °C/min (A), 10 °C/min (B), 20 °C/min (C), 30 °C/min (D), and 50 °C/min (E). Each freezing run was repeated 4 times (I–IV). In (C), the bottom graph is an overlay of cycle IV on cycle I. The hatched area is the contribution of IIF to the exotherm in Cycle I.

ing cycles at a given cooling rate and (B) the cooling rate for each cycle. Table 3 summarizes the mean values of these fractions and their standard errors. Let's first examine the extreme cases in the top plot, A; i.e., the IIF fraction for yeast cells cooled at 2 and 100 °C/min. At 2 °C/min, the IIF fraction is near zero in the first freeze cycle and remains at or near zero with each repeated freeze cycle. In other words with this low cooling rate, there is little or no IIF. In contrast, when the cells are cooled at 100 °C/min, 43% of the

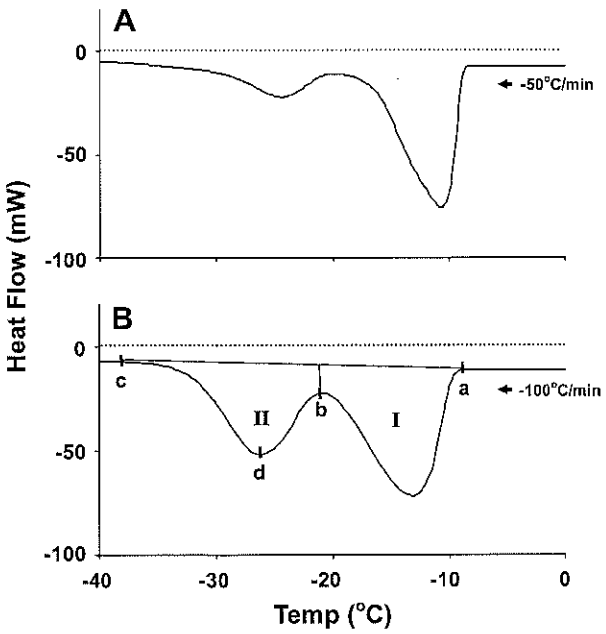

Fig. 6. DSC thermograms of yeast cells in distilled water cooled at 50 °C/min (A) and 100 °C/min (B). The bottom figure illustrates the procedure used to calculate the area of the exotherm attributable to IIF. Peak I is a portion of the exotherm produced by EIF. Peak II is a portion of the exotherm attributable to IIF. The two overlap. The area under line **bc** is considered due to IIF. A hidden tail to the right of **b** under Peak I is also attributable to IIF, but that is counterbalanced by a hidden tail under peak II that is also additive to the EIF under Peak I. If the areas of Peaks I and II are approximately equal, then the two tails should approximately cancel out. The total freezing exotherm (IIF + EIF) is the area under line **ac**. Point **d** is taken to be the modal intracellular ice nucleation temperature of the cells.

total exotherm derives from IIF on the first freeze; however, that fraction drops to 6% on the second freeze and to zero on the third freeze. For the intermediate cooling rates (5–50 °C/min), the IIF fraction or ratio behaves in an intermediate fashion. That is, the IIF fraction during the first freeze increases progressively as the cooling rate is increased from 5 to 50 °C/min.

The most instructive curve in the lower plot B is that for the first cycle since that represents the degree of IIF and presumptive lethality in the initial freezing. We see that there is a rapid linear increase in the fraction of the heat release ascribable to IIF from 9 to 43% over the cooling rate range of 10–100 °C/min. One would expect a corresponding decrease in survival over this cooling rate range.

Discussion

In order for a cell to freeze intracellularly in a distinct and separate fashion from the freezing of the external medium, the cell must be a separate compartment from the external medium. This is tantamount to saying that it must be separated from ice in the external medium by an intact plasma membrane so that the cell contents can supercool even in the presence of external ice.

IIF almost invariably disrupts the plasma membrane. For example, if it has formed during cooling, most cells are no longer osmotically responsive after thawing. Since at that point, that cell is no longer a separate compartment, it will undergo no supercooling if it is subjected to a second cycle of freezing; rather, external ice will simply grow through the cell as though it were part of the medium. The two criteria for the occurrence of IIF in this study were then (1) the occurrence in the first freeze of an exotherm at a temperature below the exotherm attributable to the freezing of the medium and (2) the diminishment and disappearance of the low temperature exotherm with repeated freezing. Based on these two criteria, we draw the following conclusions

(1) The first indication of IIF occurs at a cooling rate of 20 °C/min
(2) The fraction of the cell water that freezes intracellularly increases as the cooling rate increases from 20 to 100 °C/min. We can not distinguish the case where all the water freezes intracellularly in say 50% of the cells and none freezes in the other half from the case where 50% of the water freezes intracellularly in all of the cells.

When 1 g H_2O freezes at 0 °C, it releases 330.5 J (79 cal). We observed a mean total heat release (L_f) of 217 ± 1 J/g of sample. One contributor to the discrepancy is that our 1 g sample is only about 90% water. (The cell volume is 99 μm^3 [9]; 82% of that is water [11]) If the sample were water only, the observed L_f would increase to 256 J/g. Second, the heat of fusion decreases with temperature by approximately the difference in the specific heats of ice and water; namely, 0.5 cal/g/°C or 2 J/g/°C [10], Eq. 27]. Since IIF occurred over the range of −20 °C to −35 °C (Fig. 6), the energy released in that peak may represent the freezing of a somewhat higher mass of water than would be calculated from the value of L_f at 0 °C.

Table 3 indicates that the heat released during the IIF of yeast cooled at 100 °C/min was 43% of the total exotherm (IIF + EIF). Our parallel measurements yielded a mean cytocrit of 79% in the samples. Since 82% of the yeast cell is water, this means that 65% of the total water in the slurry was cell water. If all of this

Table 2
Area under the freezing exotherms of yeast cooled at 2, 20, and 50 °C/min.

Cooling rate	Freezing cycle	Total area of exotherms	Area under peak or shoulder (J/g)	Peak or shoulder is due to IIF* (J/g)	Fraction of total exotherm due to IIF
2 °C/min	I	227.0	57.9	0.5	0.0022
	II	216.1	55.0	−2.4	−0.0111
	III	212.0	55.6	−1.8	−0.0085
	IV	229.8	57.4	0	0
20 °C/min	I	211.2	74.1	46.3	0.2190
	II	216.7	34.5	6.71	0.0310
	III	209.8	26.1	−1.66	−0.0079
	IV	210.0	27.8	0	0
50 °C/min	I	214.7	62.7	62.7	0.2918
	II	222.8	24.9	24.9	0.1116
	III	228.8	0	0	0
	IV	227.5	0	0	0

The values are for an individual representative run for each of the three cooling rates.
* Area of the shoulder in a cycle minus the area in Cycle IV.

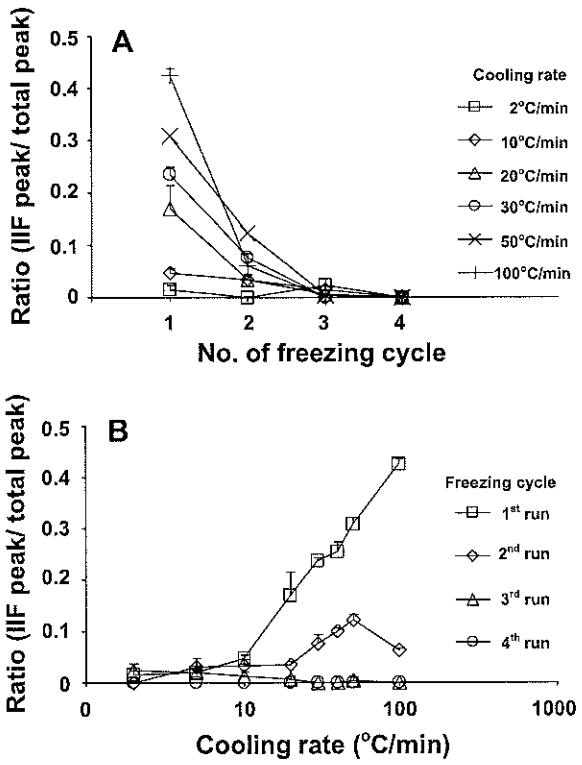

Fig. 7. Ratio of the exotherm attributable to IIF divided by the total exotherm resulting from both IIF and EIF of yeast cells suspended in distilled water and cooled at rates ranging from 2 to 100 °C/min. (A) Ratio vs. the number of times the freezing was repeated. (B) Ratio vs. the rates of cooling (logarithmic scale) in each repeated run.

Table 3
Exotherm ratios of IIF/Total.

Cooling rate (°C/min)	Freezing cycle	IIF/Total exotherm	S.E.
2 ($n = 3$)	I	0.00848	0.00732
	II	0.01104	0.01104
	III	0	0
	IV	0	0
5 ($n = 3$)	I	0.06656	0.01402
	II	0.04563	0.01869
	III	0.01928	0.00569
	IV	0	0
10 ($n = 3$)	I	0.09355	0.01039
	II	0.04554	0.00884
	III	0.01410	0.00711
	IV	0	0
20 ($n = 3$)	I	0.21080	0.04278
	II	0.03766	0.00342
	III	0.00705	0.00705
	IV	0	0
30 ($n = 4$)	I	0.236	0.007937
	II	0.075667	0.01713
	III	0	0
	IV	0	0
50 ($n = 5$)	I	0.309	0.013598
	II	0.1226	0.008931
	III	0.005	0.005
	IV	0	0
100 ($n = 3$)	I	0.42667	0.011348
	II	0.06282	0.005568
	III	0	0
	IV	–	–

cell water froze intracellularly with a cooling rate of 100 °C/min, the exotherm in Peak II should have been 143 J/g of sample out of the total of 220 J/g released. The actual heat in the IIF peak was 0.427 × 220 (Table 3) or 92.4 J/g of sample. This arithmetic indicates that 92.4/143 or 64% of the cell water froze intracellularly in cells cooled at 100 °C/min. The other 36% flowed out of the cells during cooling and froze extracellularly.

Experimental observations on IIF from DSC vs. predictions from modeling

The predictions from the modeled curves in Fig. 3 fall into three groups, depending on cooling rate. The first prediction is that yeast cells cooled at 2, 5, and 10 °C/min should not undergo IIF. The reason is that they have shrunken to equilibrium by −10 to −16 °C, some 10° or more above the temperature at which IIF becomes possible. By definition, if they are at equilibrium, they are not supercooled, and freezing can not occur in the absence of supercooling. This prediction is in accord with the DSC measurements. The second group of predictions is that cells cooled at 30, 50, or 100 °C/min should undergo IIF with near certainty. They cross the nucleation temperature of −25 °C containing far more cell water than is the case at equilibrium, and that water is supercooled over 20 °C (the horizontal distance from the curve at −25 °C to where it intersects with the equilibrium curve). These predictions are also in accord with the DSC measurements. Finally, the model curve predicts that 82% of the water in the cells will freeze intracellularly when they are cooled at 100 °C/min. That is in reasonable agreement with the conclusion from the magnitudes of the experimental exotherms that 64% of the cell water froze intracellularly at that cooling rate. The agreement may actually be closer since, as discussed, water–ice exotherms below 0 °C understate the mass undergoing the phase change because the value of L_f used in the calculation is too large.

The third and final prediction concerns the yeast cells cooled at 20 °C/min. They arrive at −25 °C containing a predicted 15% of their intracellular water, and that water is supercooled about 20 °C. In 1977, Mazur [12] assumed somewhat arbitrarily that to freeze intracellularly, a cell had to contain 10% of its original water and that water needed to be supercooled 2 °C or more. Pitt and Steponkus [22] and Pitt et al. [23] reached a similar conclusion on the basis of a sophisticated probability analysis. Based on those criteria, at least some of the water in yeast cells should freeze intracellularly at a cooling rate of 20 °C/min. On the other hand, Mazur and colleagues [17] have determined that mouse oocytes do not undergo IIF if their water contents are 20% or less. Since we calculate the water content of the yeast cooled at 20 °C/min to be about 15% of normal when they arrive at −25 °C, we would predict that the cells would not freeze intracellularly. In other words, the situation at a cooling rate of 20 °C/min is border line. This too is in accord with the interpretation of the DSC data.

Factors affecting the computed curves

The two main factors affecting the shape and position of the curves in Fig. 3 are Lp and its activation energy, *Ea*. Differences in Lp shift the curves horizontally but do not change their shapes. We used a value of 0.1 μm/min/atm. If the true value were say 0.2 μm/min/atm, the curve in Fig. 3 that we have labeled 10 °C/min would then become the curve for 20 °C/min. Changes in Ea, in contrast, change the shape of the curves. We used a value of 13.5 kcal/mol. If we had used a higher value, the effect would be to make each curve bend more sharply at lower temperatures.

Effect of cooling rate on the survival of yeast cells, the computed likelihood of IIF, and the occurrence of IIF observed by DSC

As just discussed, the observed functional relationship between cooling rate and IIF agrees closely with the computed relationship. It is widely agreed that IIF is a lethal event. How then is the viability of yeast cells affected by the rate at which the cells are cooled? Like many other cell types, plots of the survival of yeast vs. cooling rate are in the form of an inverted U. Maximum survival (55%) occurs at a cooling rate of 7 °C/min; near-minimum survival (9.6%) occurs at a cooling rate of 45 °C/min with a slight further drop to 2.8% at a cooling rate of 200 °C/min. [16]. Morris et al. [19] and Dumont et al. [3] have obtained almost identical results. Thus, the drop in viability occurs over almost exactly the same cooling rate range as the predicted and observed occurrence of IIF.

Consequently, these comparisons and the modeling and DSC experiments reported here make cells of the yeast *S. cerevisiae* the second case where a full triad of evidence demonstrates a quantitative coupling between IIF and killing and demonstrates the validity of applying fundamental physical–chemical principles to the prediction of the likelihood of IIF. The first case was the mouse oocyte/embryo. We believe it is important to complete this triad for at least several other cell types. One reason, of course, is to gain a sense of how widely these conclusions are applicable. The other reason is the opposite face of the coin. There is one prominent case (mammalian sperm) where the triad of evidence is mutually inconsistent. In sperm the cooling rates predicted to induce IIF and consequent lethality are inconsistent with those observed to cause death unless major changes in model parameters are made [15], and to date there is no direct evidence for IIF in sperm cooled at any rate [20]. Resolving these inconsistencies and determining whether they occur in still other cell types is of obvious importance to our understanding of cryobiological fundamentals and to successful cryopreservation of difficult cell types.

Acknowledgments

This work was supported by the National Institutes of Health (NIH) Grant R01-RR18470. We thank Dr. Cletus Kurtzman of NCAUR, USDA for providing the yeast culture.

References

[1] H. Bank, P. Mazur, Visualization of freezing damage, J. Cell Biol. 57 (1973) 729–742.
[2] G. Bryant, DSC measurement of cell suspensions during successive freezing runs: implications for the mechanisms of intracellular ice formation, Cryobiology 32 (1995) 114–128.
[3] F. Dumont, P.-A. Marechal, P. Gervais, Influence of cooling rate on *Saccharomyces cerevisiae* destruction during freezing: unexpected viability at ultra-rapid cooling rates, Cryobiology 46 (2003) 33–42.
[4] X. Han, D. Luo, X. Cui, S. Heimfeld, D. Gao, A modified differential scanning calorimetry method for determining water transport properties in biological cells during the freezing process, Cell Preserv. Technol. 5 (2007) 25–32.
[5] H.J. Hinz, F.P. Schwarz, Measurement and analysis of results obtained on biological substances with differential scanning calorimetry (IUPAC Technical Report), Pure Appl. Chem. 73 (2001) 745–759.
[6] F.W. Kleinhans, J.F. Guenther, D.M. Roberts, P. Mazur, Analysis of intracellular ice nucleation in Xenopus oocytes by differential scanning calorimetry, Cryobiology 52 (2006) 128–138.
[7] R.L. Levin, Water permeability of yeast cells at sub-zero temperatures, J. Membr. Biol. 46 (1979) 91–124.
[8] P. Mazur, Physical and temporal factors involved in the death of yeast at subzero temperatures, Biophys. J. 1 (1961) 247–264.
[9] P. Mazur, Manifestations of injury in yeast cells exposed to subzero temperatures, II. Changes in specific gravity and in the concentration and quantity of cell solids, J. Bacteriol. 82 (1961) 673–684.
[10] P. Mazur, Kinetics of water loss from cells at subzero temperatures and the likelihood of intracellular freezing, J. Gen. Physiol. 47 (1963) 347–369.
[11] P. Mazur, Studies on rapidly frozen suspensions of yeast cells by differential thermal analysis and conductometry, Biophys. J. 3 (1963) 323–353.
[12] P. Mazur, The role of intracellular freezing in the death of cells cooled at supraoptimal rates, Cryobiology 14 (1977) 251–272.
[13] P. Mazur, Principles of cryobiology, in: B.J. Fuller, N. Lane, E.E. Benson (Eds.), Life in the Frozen State, CRC Press, Boca Raton, Fl, 2004, pp. 3–65.
[14] P. Mazur, W.F. Rall, S.P. Leibo, Kinetics of water loss and the likelihood of intracellular freezing in mouse ova: influence of the method of calculating the temperature dependence of water permeability, Cell Biophys. 6 (1984) 197–213.
[15] P. Mazur, C. Koshimoto, Is intracellular ice formation the cause of death of mouse sperm frozen at high cooling rates?, Biol Reprod. 66 (2002) 1485–1490.
[16] P. Mazur, J.J. Schmidt, Interactions of cooling velocity, temperature, and warming velocity on the survival of frozen and thawed yeast, Cryobiology 5 (1968) 1–17.
[17] P. Mazur, I.L. Pinn, F.W. Kleinhans, Intracellular ice formation in mouse oocytes subjected to interrupted rapid cooling, Cryobiology 55 (2007) 158–166.
[18] J.L. McNaughton, C.T. Mortimer, Differential Scanning Calorimetry, IRS Physical Chemistry Series 2vol 10, Butterworths, London, 1975. Reprinted by Perkin–Elmer, # L-604.
[19] G.J. Morris, G.E. Coulson, K.T. Clarke, Freezing injury in *Saccharomyces cerevisiae*. The effect of growth conditions, Cryobiology 25 (1988) 471–482.
[20] G.J. Morris, Rapidly cooled human sperm: no evidence for intracellular ice formation, Human Reprod. 21 (2006) 2075–2083.
[21] T. Nei, Structure and function of frozen cells: freezing patterns and post-thaw survival, J. Microsc. 112 (1978) 197–204.
[22] R.E. Pitt, P.L. Steponkus, Quantitative analysis of the probability of intracellular ice formation during freezing of isolated protoplasts, Cryobiology 26 (1989) 44–63.
[23] R.E. Pitt, S.P. Myers, T.-T. Lin, P.L. Steponkus, Subfreezing volumetric behavior and stochastic modeling of intracellular ice formation in *Drosophila melanogaster* embryos, Cryobiology 28 (1991) 72–86.
[24] M.W. Scheiwe, C. Körber, Basic investigations on the freezing of human lymphocytes, Cryobiology 20 (1983) 257–273.
[25] G.J. Schwartz, K.R. Diller, Osmotic response of individual cells during freezing II. Membrane permeability analysis, Cryobiology 20 (1983) 542–552.
[26] M. Shabana, J.J. McGrath, Cryomicroscope investigation and thermodynamic modeling of the freezing of unfertilized hamster ova, Cryobiology 25 (1988) 338–354.